Contents lists available at SciVerse ScienceDirect

Journal of Theoretical Biology

journal homepage: www.elsevier.com/locate/yjtbi

Spatial instabilities untie the exclusion-principle constraint on species coexistence

Jonathan Nathan [a,*], Ehud Meron [a,b], Jost von Hardenberg [c]

[a] Department of Solar Energy and Environmental Physics, BIDR, Ben Gurion University, Sede Boker Campus 84990, Israel
[b] Department of Physics, Ben Gurion University, Beer Sheva 84105, Israel
[c] ISAC-CNR, Corso Fiume 4, I-10133 Torino, Italy

HIGHLIGHTS

- Spatial patterns allow coexistence of two species, competing on one resource.
- Competition increases the precipitation range that supports spatial patterns.
- Invasion of a strong competitor can drive a patterned system to extinction.

ARTICLE INFO

ABSTRACT

Using a spatially explicit mathematical model for water-limited vegetation we show that spatial instabilities of uniform states can lead to species coexistence under conditions where uniformly distributed species competitively exclude one another. Coexistence is made possible when water-rich patches formed by a pattern forming species provide habitats for a highly dispersive species that is a better competitor in uniform settings.

© 2013 Elsevier Ltd. All rights reserved.

1. Introduction

Species coexistence and diversity are fundamental aspects of community dynamics widely explored in the context of resource-limited ecosystems (Shmida and Ellner, 1984; Chesson, 2000; Levin, 2000; Turchin, 2003; Herben and Hara, 2003; Scheiter and Higgins, 2007; Pronk et al., 2007; Nevai and Vance, 2007; May et al., 2009; Díaz-Sierra et al., 2010). One of the main theoretical results is the competitive exclusion principle, stating that two species competing for the same limiting resource cannot coexist if other ecological factors are constant (Hardin, 1960). This easily verifiable mathematical statement rarely holds in real ecosystems, which are often characterized by a wide abundance of different species, apparently exploiting the same limiting

resource. Many mechanisms have been suggested to explain this discrepancy between theory and reality, including niche differentiation due to heterogeneous space and time (Goldberg and Novoplansky, 1997; Tilman, 1994; Amarasekare, 2003), species specific predation (Takeuchi and Adachi, 1984; Hulme, 1996), species that affect each other directly (Vance, 1984) and others. All these explanations make a step towards reality in breaking the main assumption of the exclusion principle – uniform environmental conditions and similar species behavior in all aspects beside competition on a resource (Barot, 2004).

Despite the significance of environmental heterogeneity for species diversity, studies of species coexistence have largely overlooked an important driver of such heterogeneity – spatial instabilities leading to *self-organized* patchiness (Gilad et al., 2007a; Meron, 2012). A well studied context of such patchiness is vegetation pattern formation in water limited ecosystems (Deblauwe et al., 2008). Model studies of water-limited ecosystems have identified local biomass-water feedbacks capable of inducing instabilities of uniform vegetation that result in global

* Correspondence to: Blaustein Institutes for Desert Research, Ben Gurion University, Beer Sheva 84105, Israel. Tel.: +972 8 6461853; fax: +972 8 6472904.
E-mail addresses: nathanj@post.bgu.ac.il (J. Nathan), ehud@bgu.ac.il (E. Meron), j.vonhardenberg@isac.cnr.it (J. von Hardenberg).

regular and irregular vegetation patterns (Rietkerk et al., 2002; Barbier et al., 2006; Gilad et al., 2007b; von Hardenberg et al., 2010). These patterns can form even in the absence of any environmental heterogeneity, such as micro-topography or differences in soil type.

Associated with vegetation pattern formation are resource redistribution and ecosystem engineering, which may affect inter-specific interactions (Gilad et al., 2004, 2007b). Studies of a two species model representing a water-limited woody-herbaceous system with a pattern-forming woody engineer, have demonstrated transitions from competition and exclusion of the herbaceous life form at high rainfall to facilitation and coexistence at low rainfall (Gilad et al., 2007a), consistently with field observations (Holzapfel et al., 2006). These studies, however, assumed the existence of a maximal standing biomass, a parameter representing constraints on above-ground biomass growth such as plant-shoot architecture. This assumption, which breaks the conditions of the exclusion principle, allows for species coexistence even in uniform systems. In this paper we study whether self-organized patchiness alone can induce species coexistence. That is, we consider a system that satisfies all the assumptions of the exclusion principle, except that it is spatially extended. We show that although the system's environment is assumed to be homogeneous, spatial instabilities leading to patterned states can induce species coexistence. This result is implicit in a recent study on savanna ecosystems (Baudena and Rietkerk, 2013), but has not been spelled out. We further show various realizations of species exclusion and coexistence, and we uncover the conditions that are required to yield these realizations.

2. The model

Vegetation pattern formation in drylands has been studied using a wide range of mathematical models (see for example Borgogno et al., 2009; Lefever and Lejeune, 1997; O. Lejeune and Lefever, 2004; Rietkerk et al., 2002; Gilad et al., 2004). While representing the soil-vegetation-atmosphere feedbacks at different degrees of detail, most models produce the same basic characteristics of vegetation patchiness, including the sequence of vegetation states (uniform and patterned) along environmental gradients, and bistability ranges between any consecutive pair of vegetation states. This is largely due to the universal behavior of dynamical systems near instability points. The relevant instability in the present case is a stationary nonuniform instability of a uniform vegetation state, which leads to stripe patterns and two forms of hexagonal patterns (Cross and Greenside, 2009), representing spot and gap patterns.

A similar degree of universality is expected in models for two competing species. We therefore use a fairly simplified version of the model which was introduced in Gilad et al. (2007a) and Meron (2011) for a pattern-forming species and a non-pattern forming species that compete for a single limiting resource – soil water. We first omit the maximum standing biomass limitation to regain the validity of the exclusion principle in the absence of a pattern forming instability. This will allow us later on to attribute species coexistence to spatial self organization. We further keep only one pattern forming feedback – a larger infiltration rate of surface water into vegetated soil compared to bare soil, dropping the positive feedback associated with root-shoot relations (Gilad et al., 2007b). An additional simplification is the replacement of the nonlinear diffusion term in the equation for the surface-water variable by a linear diffusion term, as we will further explain below. Under these simplifications the model can be regarded as an extension of the model introduced by HilleRisLambers et al. (2001) to two species.

The simplified model version reads

$$\partial_t B_1 = (C_1 W - M_1) B_1 + D_1 \nabla^2 B_1$$
$$\partial_t B_2 = (C_2 W - M_2) B_2 + D_2 \nabla^2 B_2$$
$$\partial_t W = J(B_1) H - W(N + \Gamma_1 B_1 + \Gamma_2 B_2) + D_W \nabla^2 W$$
$$\partial_t H = P - J(B_1) H + D_H \nabla^2 H \tag{1}$$

with $J(B_1) = A(B_1 + Qf)/(B_1 + Q)$. The model represents vegetation densities for two species, B_i ($i=1,2$), the first pattern-forming and the second not, with growth rates C_i, mortality rates M_i, and diffusion (dispersal) rates D_i. The two species compete for a single resource, water, which is modeled by two layers. One is soil water, W, which contributes linearly to biomass growth of both species. The soil water is reduced by evaporation at a rate N and by water uptake due to each species with rates $\Gamma_i B_i$. The soil water density increases by infiltration from the surface water layer, H, at a rate $J(B_1)$. This biomass dependence simulates the higher infiltration rate in vegetated areas due to the absence of a soil crust and, in some cases, the formation of a soil mound that intercepts runoff, as explained in Gilad et al. (2007b). In principle, the infiltration rate should also depend on B_2. However, in order for B_2 to remain non-pattern forming this dependence should be weak enough and for simplicity we omit it. We verified that introducing a weak dependence on B_2, while remaining in a parameter range where B_2 alone does not form patterns, does not change our qualitative results. In the surface water equation overland water flow is represented by a simple diffusive term $\nabla^2 H$. This term, together with the $J(B_1)H$ term, is responsible for the instability to periodic vegetation patterns; the surface water flow towards vegetation patches, because of higher infiltration rates at the patch areas, provides a mechanism for short range facilitation and long-range competition that favors nonuniform vegetation. In other papers, such as Gilad et al. (2007b), a nonlinear diffusion term of the form $\nabla^2 H^2$ has been used. While this form is better motivated from a physical point of view, the linear version used here allows for a simpler numerical and analytical solution of the equations and we verified that our results do not depend crucially on this detail.

As a first step in our analysis we non-dimensionalize the equations and reduce the parameter space, using the mortality, dispersal and growth rates of the first species to define scales for time, space and water, respectively, and using the soil–water uptake rates of both species to rescale their biomasses

$$\partial_t b_1 = (w-1) b_1 + \nabla^2 b_1$$
$$\partial_t b_2 = (c_2 w - \mu_2) b_2 + d_2 \nabla^2 b_2$$
$$\partial_t w = I(b_1) h - w(n + b_1 + b_2) + d_w \nabla^2 w$$
$$\partial_t h = p - I(b_1) h + d_h \nabla^2 h, \tag{2}$$

where $I(b_1) = \alpha(b_1 + qf)/(b_1 + q)$, $\alpha = A/M_1$, $n = N/M_1$, $p = PC_1/M_1^2$, $\mu_2 = M_2/M_1$, $c_2 = C_2/C_1$ $d_2 = D_2/D_1$, $d_w = D_W/D_1$, $d_h = D_H/D_1$, $q = Q\Gamma_1/M_1$ $b_1 = B_1\Gamma_1/M_1$, $b_2 = B_2\Gamma_2/M_1$, $w = WC_1/M_1$, $h = HC_1/M_1$, $x = \sqrt{M_1/D_1}X$, $t = M_1 T$.

We study solutions of these model equations for different parameter values, addressing the question how pattern formation affects the community dynamics of the two competing species. We will limit our analysis to one-dimensional systems and concentrate on the parameters which control water stress and competition. These are the precipitation rate p and the parameters defining the second species, c_2, μ_2, d_2. The parameters n, α, q, f, d_w and d_h, which control soil water dynamics and overland flow are kept constant and appropriate values to represent dryland water-vegetation interactions are chosen. The specific values we choose, $\alpha = 40$, $q = 0.1$, $f = 0.1$, $n = 1$, $d_w = 100$, $d_h = 10\,000$, have been employed and discussed in Gilad et al. (2004, 2007b). We fix the non-dimensional domain size to 400, equivalent to a domain of $D \approx 9.1$ m in dimensional units when realistic values are chosen for the dimensional parameters. The parameters c_2 and μ_2 both

regulate the growth rate of the second species and we verified that varying either of them has almost the same qualitative effect in terms of the results described below. We therefore set $\mu_2 = 1$, which reduces the control parameter space to (p, c_2, d_2).

3. Results

3.1. No species interaction

We consider first the model equations for a single species by setting the biomass of the other species identically to zero. The simplest solutions of the single-species model describe stationary uniform states. One solution of this kind describes bare soil. The solution is stable up to a critical precipitation value $p = p_{bi}$, where $p_{b1} = n$ for the first species and $p_{b2} = n\mu_2/c_2$ for the second (hereafter we refer to the two species through their biomass variables b_1 and b_2). The critical value designates a uniform stationary instability (transcritical bifurcation) at which uniform perturbations begin to grow monotonically in time. In the case of b_2 the instability leads to a stationary uniform vegetation state, which is stable for all $p > p_{b2}$, as the bifurcation diagram in Fig. 1 indicates. The case of b_1 is more intricate as the stationary uniform vegetation state that appears at $p = p_{b1}$ is unstable to the monotonic growth of nonuniform perturbations, leading to the emergence of stationary periodic patterns. This instability, associated with the infiltration feedback, occurs at high precipitation as p is decreased below a threshold value p_{pat}, whose analytical expression is too long to display here; for the parameter values used in the following simulations it is equal to 1.23. A bifurcation diagram showing the two uniform solutions and a solution branch representing a periodic pattern is shown in Fig. 2. The periodic pattern branch, calculated by a numerical continuation method using AUTO (Doedel, 1981), extends to low precipitation values and appears to terminate on the uniform vegetation branch at $p = p_{b1}$. The two instability points on the uniform vegetation branch at $p = p_{b1}$ and at $p = p_{pat}$ represent subcritical bifurcations; the stable periodic solution extends to values $p_{low} < p_{b1}$ and $p_{high} > p_{pat}$ at which pairs of stable-unstable periodic patterns appear in fold bifurcations (see Fig. 2). The ranges $p_{low} < p < p_{b1}$ and $p_{pat} < p < p_{high}$ are bistability ranges of bare soil and periodic patterns and of uniform vegetation and periodic patterns, respectively. There are many additional periodic solutions with close
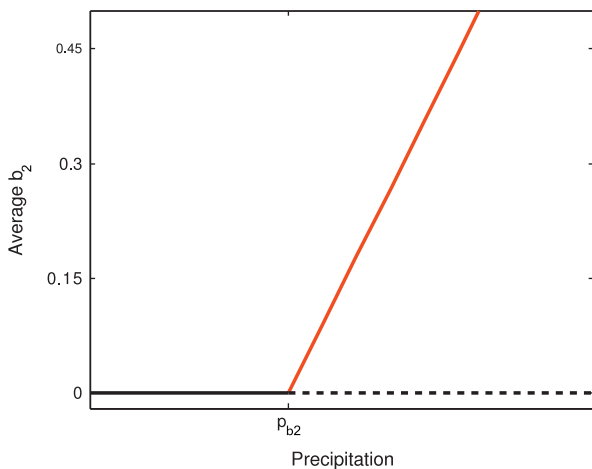
Fig. 1. Bifurcation diagram for a non-pattern-forming species (b_2). The bare-soil state (black line) loses stability to a uniform b_2 state (red line) when the precipitation p exceeds the threshold value $p_{b2} = n\mu_2/c_2$. Solid (dashed) lines represent stable (unstable) states. Parameters used: $c_2 = 1.2$, $\alpha = 40$, $q = 0.1$, $f = 0.1$, $n = 1$, $d_w = 10^2$, $d_h = 10^4$. (For interpretation of the references to color in this figure caption, the reader is referred to the web version of this article.)
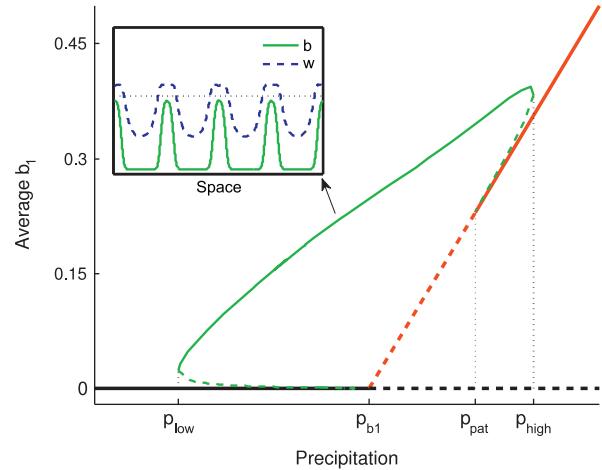
Fig. 2. Bifurcation diagram for a pattern-forming species (b_1). The diagram shows three solution branches representing bare soil (black line), uniform b_1 (red line), and a periodic b_1 patterns (green line). The periodic pattern solution appears in a pair of subcritical instabilities that result in two bistability ranges: bare soil and periodic b_1 pattern $p_{low} < p < p_{b1}$, and uniform b_1 and periodic b_1 pattern $p_{pat} < p < p_{high}$. The vertical axis represents spatial biomass average. The inset shows the spatial biomass and soil–water distributions at $p = 0.88$. For reference, the dotted line represents the equilibrium soil–water level corresponding to bare soil. Parameters used: $\alpha = 40$, $q = 0.1$, $f = 0.1$, $n = 1$, $d_w = 10^2$, $d_h = 10^4$. (For interpretation of the references to color in this figure caption, the reader is referred to the web version of this article.)

wavenumbers and with overlapping ranges of stability, but for simplicity in the following we focus only on solutions with four vegetation patches.

The inset of Fig. 2 shows the spatial profiles of the biomass and soil–water variables associated with the periodic solution. The dotted line shows the soil–water level of the uniform bare-soil solution. Notice the correlation between the biomass and the soil water profiles; the higher soil–water content at vegetation patches is a consequence of the infiltration feedback which induces overland flow towards the patches. This may not be the case if the root-shoot feedback (Gilad et al., 2007b) is kept in the model: The root-shoot feedback counteracts the infiltration feedback by depleting the soil–water content under a vegetation patch. When sufficiently strong, it may shift the balance between the two feedbacks to form anti-correlated biomass and soil–water distributions (Gilad et al., 2004, 2007b; Meron et al., 2007). Note also that for $p < p_{b1}$ and the chosen parameters the soil water content in a vegetation patch is higher than the content associated with the bare soil state (dotted line). This means that in forming water-rich patches the pattern-forming species act as an ecosystem engineer.

3.2. Two species competition and coexistence

When both species are allowed to compete, a richer picture emerges. There are four stationary uniform solutions: bare soil ($b_1 = 0$, $b_2 = 0$), uniform b_1 ($b_1 \neq 0$, $b_2 = 0$), uniform b_2 ($b_1 = 0$, $b_2 \neq 0$), and uniform coexistence ($b_1 \neq 0$, $b_2 \neq 0$). The latter, however, exists only for parameter values for which $\mu_2/c_2 = 1$. In fact, there is a continuous family of coexistence solutions given by $b_1 + b_2 = p - n$. The constraint $\mu_2/c_2 = 1$ corresponds to two highly similar species, having possibly different dispersal rates, but characterized by the same equilibrium value of the resource, $w = \mu_2/c_2 = 1$. This is a non-generic case, unexpected to be observable in practice. As often discussed in the literature, only states existing over a finite parameter range are expected to be observable (Meszena et al., 2006). When μ_2/c_2 deviates from unity, the only non-zero stable uniform solutions are those involving the

exclusion of one species, i.e. uniform b_1 or uniform b_2, consistently with the competitive exclusion principle for a single limiting resource. In this case the value of w associated with these single-species solutions plays the role of the equilibrium value of the resource, R^*, introduced, among others, by Tilman (1982).

The existence and stability ranges of the other three stationary uniform solutions can be obtained performing a linear stability analysis of Eqs. (2). The bare soil state is given by $b_1 = 0$, $b_2 = 0$, $w = p/n$, $h = p/(\alpha f)$. It is stable at low precipitation rates and loses stability to the growth of b_1 at $p_{b1} = n$ when $\mu_2/c_2 > 1$, and to the growth of b_2 at $p_{b2} = \mu_2 n/c_2$ when $\mu_2/c_2 < 1$. The uniform b_1 solution is given by $b_1 = p - n$, $b_2 = 0$, $w = 1$, $h = p/I(b_1)$. It is stable at high p and low c_2 and loses stability to the growth of non-uniform perturbations as p decreases below a certain threshold, $p_{pat} = 1.23$ for the parameters used in this study, and to the growth of b_2 as c_2 exceeds μ_2. The uniform b_2 solution is given by $b_1 = 0$, $b_2 = p(c_2/\mu_2) - n$, $w = \mu_2/c_2$, $h = p/(\alpha f)$. It is stable at high p and high c_2 and loses stability to bare soil as p decreases below the threshold $p_{b2} = \mu_2 n/c_2$, and to the growth of b_1 as c_2 decreases below μ_2. Note that the results for the thresholds p_{b1}, p_{b2} and p_{pat} coincide with those obtained for the single-species model (see Section 3.1 and Fig. 2). Together with the threshold $c_2 = \mu_2$ they define boundary lines in the (p, c_2) parameter plane that separate domains of different stable uniform states:

(1) *Uniform b_1*: ($p > p_{pat}$ and $c_2 < \mu_2$).
(2) *Uniform b_2*: ($p > p_{b2}$ and $c_2 > \mu_2$).
(3) *Bare soil*: ($p < p_{b1}$ and $c_2 < \mu_2$), ($p < p_{b2}$ and $c_2 > \mu_2$).

The domains described above leave out uncovered the domain ($p_{b1} < p < p_{pat}$ and $c_2 < \mu_2$), where no stable uniform states exist and stable periodic b_1 patterns prevail.

The picture, however, is far richer because of the existence of nonuniform states whose stability domains overlap with those of the uniform states, as the state diagram in Fig. 3 shows. The uniform states in this diagram occupy the colored domains 1–3, delimited by the dashed lines, which denote the stability boundaries presented above. The additional colored domains denote alternative non-uniform stable states, among them *patterned states of species coexistence*.

The stable periodic b_1 patterns in domain ($p_{b1} < p < p_{pat}$ and $c_2 < \mu_2$) (designated 4b in Fig. 3) extend also to the range $p_{low} < p < p_{high}$, as in the single species problem (see Fig. 2). This implies bistability domains of bare soil and periodic b_1 patterns (4a), and of uniform b_1 and periodic b_1 patterns (4c). The domain of stable periodic b_1 patterns also extends to c_2 values above μ_2. This results in bistability of uniform b_2 and periodic b_1 patterns.

A further detail is that there exists a family of stable periodic b_1 patterns in domain 4 with different wavenumbers, some of them extending to other domains as will be discussed in Section 3.3 in the context of state transitions induced by an invading b_2 species.

Two additional bistability domains of uniform and nonuniform states exist (domains 5 and 6 in Fig. 3). In both domains the nonuniform state is spatially periodic and involves both species, however in domain 5 the pattern is stationary whereas in domain 6 it is oscillatory. The alternative stable state in both domains for $p > p_{high}$ is uniform b_2. Below p_{high} periodic b_1 patterns are also alternative stable states, and below p_{b2} bare soil becomes an alternative stable state instead of uniform b_2. Two factors are responsible for this coexistence. The first is the capability of b_1 to act as an ecosystem engineer, i.e. the capability to increase the soil water content in its patch areas beyond the level of bare soil (see Fig. 2). Such patches create new niches for b_2 that favor species coexistence. This factor alone, however, cannot induce stable species coexistence because of the local competitive advantage
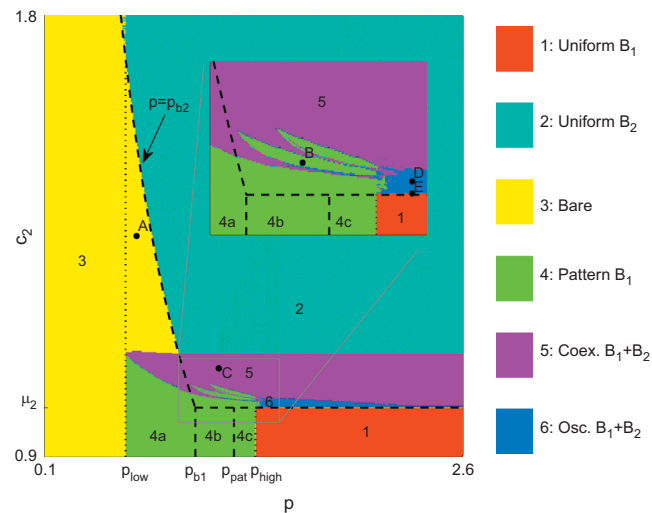
Fig. 3. State diagram showing domains of different states in the parameter plane spanned by p and c_2. The dashed lines denote the stability boundaries of bare soil ($p = p_{b1} = n$ and $p = p_{b2} = n\mu_2/c_2$), uniform b_1 ($p = p_{pat} = 1.23$ and $c_2 = \mu_2$), and uniform b_2 ($p = p_{b2}$ and $c_2 = \mu_2$). The dotted lines are the boundaries $p = p_{low}$ and $p = p_{high}$ of a stable periodic b_1 pattern. The colors denote different asymptotic states according to the legend on the right. The black circles refer to the dynamical behavior described in Figs. 4–7. The states appearing in the map where obtained by following the solutions along the c_2-axis in a stepwise manner, were the initial condition in each step is the asymptotic solution of the previous step subjected to random perturbations. The inset shows a blow up of the designated rectangular area where invasion-type initial conditions have been used. The latter better reveal the intricate structure of periodic b_1 solutions of increasing wavenumbers. The parameter values are as indicated in the model description and $d_2 = 10$. (For interpretation of the references to color in this figure caption, the reader is referred to the web version of this article.)

of b_2; the growth of b_2 can lead to the local extinction of b_1 and of the niches it creates. The additional factor that is needed for stable coexistence is a higher dispersal rate of b_2. In patchy and fragmented environments high dispersal rate has a negative effect on the growth within the patch since much of the reproductive effort is wasted on non-productive areas such as the water deficient soil located between patches. In that case, the b_2 growth within the patch will be limited by the strong dispersion outwards, allowing it to coexist with b_1 for a range of $c_2 > \mu_2$. We have verified that the width of this range increases for increasing d_2.

3.3. Invasion induced dynamics

The multiplicity of stable states allows for interesting dynamical behavior involving state transitions which we explore in the context of a species invasion problem. That is, we study the responses of well established b_1 populations to the local invasion of b_2. To study such responses we consider periodic or uniform initial conditions for b_1, and a small hump-shape initial perturbation for b_2 centered at one of the b_1 patches. The periodic initial conditions for b_1 are obtained by solving the single-species model.

Consider first a stationary periodic b_1 pattern in the range $p_{low} < p < p_{b2}$ of domain 4 where bare soil is an alternative stable state. Consider further a local invasion of a fast growing b_2 species with $c_2 > \mu_2$ (point A in Fig. 3). The dynamics that result from such an initial condition is shown in Fig. 4. The water-rich b_1 patch provides favorable conditions for the growth of b_2, which out competes b_1 and leads to its local extinction. Diffusion of b_2 induces the same process in the nearby b_1 patches, leading eventually to the extinction of both species and to the convergence to the alternative stable state – the bare soil.

A different process occurs with a further decrease of c_2 and an increase of p (point B in Fig. 3). Under these conditions the local
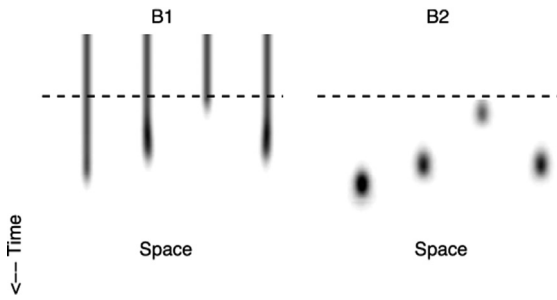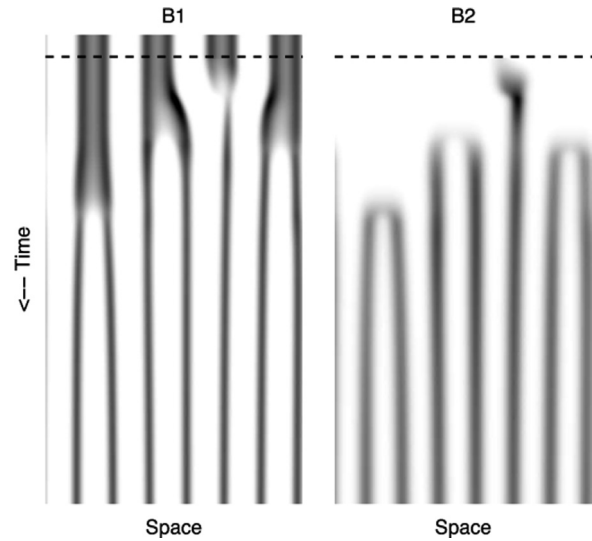
Fig. 4. Space–time plot describing a transition from a b_1 pattern to bare soil induced by a local invasion of b_2. The dashed line denotes the introduction time of b_2. Darker shades denote higher biomass. The parameters correspond to point A in Fig. 3.
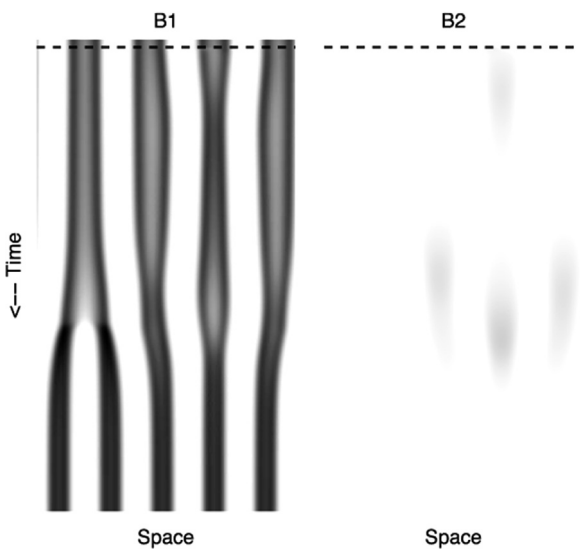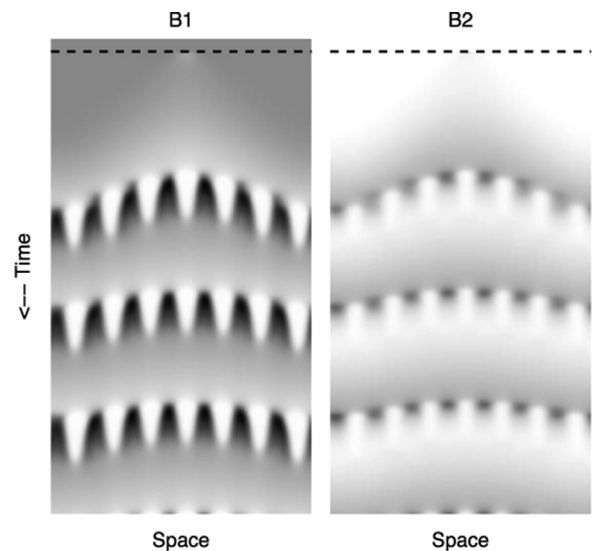

Fig. 5. Space–time plot describing a transition from one b_1 pattern to another that involves wavenumber increase. The transition is induced by local b_2 invasion which goes extinct in the course of the transition. The dashed line denotes the introduction time of b_2. Darker shades denote higher biomass. The parameters correspond to point B in Fig. 3.

Fig. 6. Space–time plot describing a transition from a b_1 pattern to a stationary coexistence pattern involving both b_1 and b_2. The transition is induced by local b_2 invasion. The dashed line denotes the introduction time of b_2. Darker shades denote higher biomass. The parameters correspond to point C in Fig. 3.

Fig. 7. Space–time plot describing a transition from a uniform b_1 state to an oscillatory coexistence pattern involving both b_1 and b_2. The transition is induced by local b_2 invasion. The dashed line denotes the introduction time of b_2. Darker shades denote higher biomass. The parameters ($p = 1.46$ and $c_2 = 1.01$) correspond to point D in Fig. 3.

introduction of b_2 in a b_1 patch can no longer lead to patch extinction, but does reduce its size. This in turn allows the adjacent patches of b_1 to grow larger, and possibly split into two patches. The denser b_1 pattern that results forms unfavorable conditions for the growth of b_2 and leads to a periodic b_1 pattern of higher wavenumber as Fig. 5 demonstrates. This scenario of wavenumber increase occurs in a band-like domain in the (c_2, p) plane as shown in the inset of Fig. 3. At higher c_2 the same scenario leads to a b_1 pattern with a yet higher wavenumber (the upper band-like domain in Fig. 3).

In the examples described above the overall role of b_2 was to trigger a transition from one stable state to another both of which do not involve b_2. Repeating the numerical invasion experiment in domain 5 (at point C in Fig. 3) leads to an early stage behavior similar to that found at point B (Fig. 5), in that the invaded b_1 patch shrinks in size and allows the adjacent patches to grow and split. This time, however, the invading b_2 species does not go extinct but rather persists and keeps invading all other b_1 patches to form a coexistence pattern. The difference with respect to the behavior at point B is that the b_1 patch splitting occurs across the whole pattern, doubling the pattern's wavenumber in this case. As a consequence, the b_1 patches are much smaller and while they are

still active in increasing the infiltration rate of surface water, their water consumption is much reduced, thereby creating favorable conditions for b_2.

So far we discussed the local invasion of b_2 into a b_1 pattern. Fig. 7 shows the result of a numerical experiment where b_2 invades a uniform b_1 state (point D in Fig. 3). In this case the uniform b_1 state is unstable to the growth of b_2 perturbations (but is stable in the absence of b_2, i.e. in the single-species model for b_1). As the figure shows, the invasion results in an oscillatory coexistence pattern (occupying domain 6 in the state diagram of Fig. 3). This pattern appears in a Hopf bifurcation from the stationary coexistence pattern that exists in domain 5. As c_2 is decreased towards μ_2 the oscillation period becomes longer and diverges in the limit $c_2 \to \mu_2$. The oscillation period involves two main phases as Fig. 8 demonstrates: (i) a long phase in
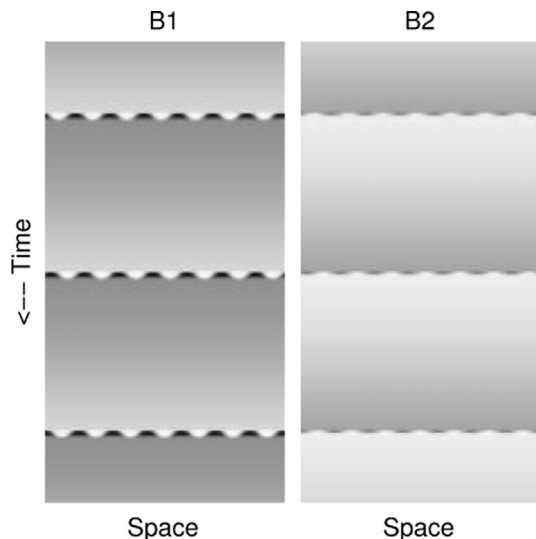
Fig. 8. Space–time plot showing the asymptotic dynamics of the oscillatory coexistence pattern in domain 6, closer to the $c_2 = \mu_2$ threshold as compared with Fig. 7. The oscillation period consists of a long, nearly uniform, phase, where the composition changes from a b_1 dominated community to a b_2 dominated community, and a short patterned phase. Darker shades denote higher biomass. The parameters ($p = 1.46$ and $c_2 = 1.001$) correspond to point E in Fig. 3.

the vicinity of the slow manifold, $b_1 + b_2 = p - n$, where the community structure is nearly uniform and slowly changes from a b_1-dominated to a b_2-dominated community, in accordance with the competitive exclusion principle and (ii) a short phase of a coexistence pattern in which the dominance of b_1 is regained. The termination of the uniform phase and the appearance of the coexistence pattern can be related to a stationary nonuniform instability of uniform coexistence states $b_1 + b_2 = p - n$ when b_1/b_2 is smaller than some threshold value.

4. Discussion

Using a spatially explicit mathematical model for plant interactions in water-limited systems, we reexamined the competitive exclusion principle under conditions where one species is capable of forming self-organized vegetation patterns. Our results suggests that even in a uniform, time-independent environment self-emergent spatial patterns can induce coexistence of two species that compete on the same resource. Exhaustive exploration of the parameter space (Fig. 3) reveals a wide range of possible dynamical behaviors.

The primary result is that introducing a second species to a water-limited system dominated by a pattern-forming species leads to wide parameter ranges where stable coexistence (in the sense of Chesson, 2000) is possible (domains 5 and 6 in Fig. 3). In these parameter ranges the pattern forming species acts as an ecosystem engineer by concentrating the water resource, while the second species, which is not pattern forming by itself, is a better competitor and characterized by a higher dispersal capability. Two forms of species coexistence were found, both representing periodic patterns with overlapping patches except that in one form the pattern is stationary (Fig. 6) and in the other it is oscillatory (Figs. 7 and 8).

It is interesting to note that this mechanism differs from the classical competition-colonization tradeoff mechanism introduced by Tilman (1994). The comparison between the two mechanisms is not straightforward since competition in Tilman's spatially implicit model is presumed and built into the model, whereas in a spatially explicit model competition is mediated by the

instantaneous spatial distribution of the limiting resource, water in our case. Moreover, colonization is interpreted differently: in Tilman's approach it is regarded as the ability to disperse and to germinate whereas in our approach it is only the ability to disperse, while germination and growth are represented separately. In fact, while in an implicit-space approach the only species property which is represented is the fraction of spatial coverage, explicit modeling of the spatial distributions adds the additional property of biomass density, allowing to separate dispersion from germination and growth. In any case, the implied result of Tilman's model is that a negative correlation between competition and colonization abilities is necessary to maintain coexistence, while we find the opposite, coexistence occurs in a range in which the better competitor is also the faster disperser. The explanation for this mismatch is that in Tilman's approach an inferior competitor species can only benefit from a higher colonization rate, while in our approach high colonization rates (i.e. biomass-diffusion rates) come at the expense of local growth. Heterogeneous soil water distribution, caused by vegetation pattern formation, can thus lead to a negative impact of a high dispersal strategy, which reduces the growth rate of the better competitor and allows the coexistence of the weaker competitor.

Two additional results are worth emphasizing. The first is the extension of the precipitation range of patterned states once the second, non-pattern forming species is introduced. While patterned states of the first species alone cease to exist above p_{high}, pattern states involving both species persist far beyond p_{high}. Spatial heterogeneity has long been recognized as a driver of species diversity (Tews et al., 2004). The result reported here suggests that the opposite may also be true; higher species diversity can increase spatial heterogeneity, forming a positive feedback loop between landscape diversity and species diversity.

The second result we wish to stress is the different invasion scenarios by which the second species can induce shifts between different states that do not involve it. The first scenario, illustrated in Fig. 4, is a transition form a patterned state of the first species to bare soil. An additional scenario is a transition that change the wavenumber of the pattern state of the first species, usually increasing it (Fig. 5). While in the first scenario the first species is vulnerable to the invasion of the second species and can go extinct, in the latter it is resilient.

Spatial patterns of species coexistence have recently been studied in the specific context of savanna ecosystems by Baudena and Rietkerk (2013) using a model with a similar mathematical formulation but in a different parameter range. As discussed above, our study focuses on the manners by which pattern formation unties the constraint of the exclusion principle on species coexistence, rather than on model applications to specific ecosystem contexts, such as savanna. Accordingly, the trait parameters that characterize the two species are quite similar and do not fit the context of tree-grass coexistence in savannas (the biomass density of the two species, for example, is quite similar as Figs. 1 and 2 imply). We believe, however, that the mechanism of species coexistence presented here applies also to the coexistence patterns found in Baudena and Rietkerk (2013). We note that the emergence of savanna landscapes as a self-organization phenomenon has been studied earlier by Gilad et al. (2007a). In that work an additional constraint has been taken into account – a maximum standing biomass – which reflects species-specific (genetic) limits on growth, such as stem strength or canopy architecture. Choosing the maximum standing biomass of the woody species to be an order of magnitude larger than that of the herbaceous species played a major role in reproducing savanna landscapes consisting of a uniform grassland interrupted by woody patches. This type of patterns differs from the patterns found in this study (and also in Baudena and Rietkerk, 2013), which are mosaics of bare-soil patches and coexistence vegetation patches.

Many of the domains depicted in the state diagram of Fig. 3 represent bistability of uniform and periodic-pattern states: domain 4a, for example, represents bistability of uniform bare soil and a periodic b_1 pattern, domain 5 represents bistability of uniform b_1 and a stationary coexistence pattern, and so on. Bistability of this kind often gives rise to a multitude of additional patterned states (Knobloch, 2008), ranging from islands of the periodic-pattern state in an otherwise uniform state (localized structures) to islands of the uniform state in an otherwise periodic pattern (hole structures). The stability of these additional states is attributed to the pinning of the transition zones (fronts) that separate areas occupied by the uniform and the periodic pattern states (Pomeau, 1986; Meron, 2012). Thus, domain 5 and possibly domain 6 too may give rise to many more coexistence patterns. We focused in this study on water-limited competition between two species, but the general results reported here are likely to be found in other communities that show spatial self-organization. Candidates for such communities include wetland vegetation (van der Valk and Warner, 2009), mussel beds (van de Koppel et al., 2008) and possibly plankton communities (Medvinsky et al., 2002). Exploring the results of multi-species competition is also very interesting and can be a goal for future studies.

Acknowledgments

References

Amarasekare, P., 2003. Competitive coexistence in spatially structured environments: a synthesis. Ecol. Lett. 6, 1109–1122.

Barbier, N., Couteron, P., Lejoly, J., Deblauwe, V., Lejeune, O., 2006. Self-organized vegetation patterning as a fingerprint of climate and human impact on semi-arid ecosystems. J. Ecol. 94 (April (3)), 537–547, URL ⟨http://doi.wiley.com/10.1111/j.1365-2745.2006.01126.x⟩.

Barot, S., 2004. Mechanisms promoting plant coexistence: can all the proposed processes be reconciled?. Oikos 106, 185–192.

Baudena, M., Rietkerk, M., 2013. Complexity and coexistence in a simple spatial model for arid savanna ecosystems. Theor. Ecol. 6 (2), 131–141.

Borgogno, F., D'Odorico, P., Laio, F., Ridolfi, L., 2009. Mathematical models of vegetation pattern formation in ecohydrology. Rev. Geophys. 47, RG1005.

Chesson, P., 2000. Mechanisms of maintenance of species diversity. Annu. Rev. Ecol. Syst. 31, 343–366.

Cross, M., Greenside, H., 2009. Pattern Formation and Dynamics in Nonequilibrium Systems. Cambridge University Press.

Deblauwe, V., Barbier, N., Couteron, P., Lejeune, O., Bogaert, J., 2008. The global biogeography of semi-arid periodic vegetation patterns. Global Ecol. Biogeogr. 17 (November (6)), 715–723, URL ⟨http://doi.wiley.com/10.1111/j.1466-8238.2008.00413.x⟩.

Díaz-Sierra, R., Zavala, M.A., Rietkerk, M., 2010. Positive interactions discontinuous transitions and species coexistence in plant communities. Theor. Popul. Biol. 77 (February (2)), 131–144, URL ⟨http://dx.doi.org/10.1016/j.tpb.2009.12.001⟩.

Doedel, E., 1981. Auto: a program for the bifurcation analysis of autonomous systems. Cong. Num. 30, 265.

Gilad, E., Shachak, M., Meron, E., 2007a. Dynamics and spatial organization of plant communities in water-limited systems. Theor. Popul. Biol. 72, 214–230.

Gilad, E., von Hardenberg, J., Provenzale, A., Shachak, M., Meron, E., 2004. Ecosystem engineers: from pattern formation to habitat creation. Phys. Rev. Lett. 93 (9), 098105.

Gilad, E., von Hardenberg, J., Provenzale, A., Shachak, M., Meron, E., 2007b. A mathematical model of plants as ecosystem engineers. J. Theor. Biol. 244, 680–691.

Goldberg, D., Novoplansky, A., January 1997. On the relative importance of competition in unproductive environments.

Hardin, G., 1960. The competitive exclusion principle. Science 131 (April), 1292–1297.

Herben, T., Hara, T., 2003. Spatial pattern formation in plant communities, Morphogenesis and Pattern Formation in Biological Systems—Experiments and Models. Springer Verlag. pp. 223–235.

HilleRisLambers, R., Rietkerk, M., van den Bosch, F., Prins, H., de Kroon, H., 2001. Vegetation pattern formation in semi-arid grazing systems. Ecology 82, 50–61.

Holzapfel, C., Tielbörger, K., Parag, H., Kigel, J., Sternberg, M., 2006. Annual plant-shrub interactions along an aridity gradient. Basic Appl. Ecol. 7, 268–279.

Hulme, P., January 1996. Herbivory, plant regeneration, and species coexistence.

Knobloch, E., 2008. Spatially localized structures in dissipative systems: open problems. Nonlinearity 21 (4), T45.

Lefever, R., Lejeune, O., 1997. On the origin of tiger bush. Bull. Math. Biol. 59, 263–294.

Levin, S.A., 2000. Multiple scales and the maintenance of biodiversity. Ecosystems 3 (November (6)), 498–506.

May, F., Grimm, V., Jeltsch, F., 2009. Reversed effects of grazing on plant diversity: the role of below-ground competition and size symmetry. Oikos 118 (January (12)), 1830–1843.

Medvinsky, A., Petrovskii, S., Tikhonova, I., Malchow, H., Li, B.-L., 2002. Spatiotemporal complexity of plankton and fish dynamics. SIAM Rev. 44, 311–370.

Meron, E., 2011. Modeling dryland landscapes. Math. Model. Nat. Phenom. 6, 163–187.

Meron, E., 2012. Pattern-formation approach to modelling spatially extended ecosystems. Ecol. Model. 234 (June), 70–82, URL ⟨http://linkinghub.elsevier.com/retrieve/pii/S0304380011003279⟩⟨http://www.sciencedirect.com/science/article/pii/S0304380011003279⟩.

Meron, E., Gilad, E., von Hardenberg, J., Provenzale, A., Schachak, M., 2007. Model studies of ecosystem engineering in plant communities, Ecosystem Engineers: Plants to Protists. Academic Press, Amsterdam, pp. 229–251.

Meszena, G., Gyllenberg, M., Pásztor, L., Metz, A., 2006. Competitive exclusion and limiting similarity: a unified theory. Theor. Popul. Theor. Popul. Biol. 69, 68–87.

Nevai, A.L., Vance, R.R., 2007. Plant interspecies competition for sunlight: a mathematical model of canopy partitioning. J. Math. Biol. 55 (June (1)), 105–145.

O. Lejeune, M.T., Lefever, R., 2004. Vegetation spots and stripes: dissipative structures in arid landscapes. Int. J. Quantum Chem. 98, 261–271.

Pomeau, Y., 1986. Front motion, metastability and subcritical bifurcations in hydrodynamics. Physica D 23, 3–11.

Pronk, T., Schieving, F., Anten, N., Werger, M., 2007. Plants that differ in height investment can coexist if they are distributing non-uniformly within an area. Ecol. Complexity 4 (4), 182–191.

Rietkerk, M., Boerlijst, M.C., van Langevelde, F., HilleRisLambers, R., van de Koppel, J., Kumar, L., Prins, H.H.T., Roos, A.M.D., 2002. Self-organization of vegetation in arid ecosystems. Am. Naturalist 160, 524–530.

Scheiter, S., Higgins, S.I., 2007. Partitioning of root and shoot competition and the stability of savannas. Am. Naturalist 170, 587–601.

Shmida, A., Ellner, S., January 1984. Coexistence of plant-species with similar niches.

Takeuchi, Y., Adachi, N., 1984. Influence of predation on species coexistence in volterra models. Math. Biosci. 70 (January (1)), 65–90.

Tews, J., Brose, U., Grimm, V., Tielbörger, K., Wichmann, M.C., Schwager, M., Jeltsch, F., 2004. Animal species diversity driven by habitat heterogeneity/diversity: the importance of keystone structures. J. Biogeogr. 31, 79–92.

Tilman, D., 1982. Resource Competition and Community Structure. Monographs in Population Biology. Princeton University Press, Princeton, New Jersey, USA.

Tilman, D., 1994. Competition and biodiversity in spatially structured habitats. Ecology 75 (1), 2–16.

Turchin, P., 2003. Evolution in population dynamics. Nature 424 (6946), 257–258.

van de Koppel, J., Gascoigne, J., Theraulaz, G., Rietkerk, M., Mooij, W., P.M.J., H., 2008. Experimental evidence for spatial self-organization and its emergent effects in mussel bed ecosystems. Science 322, 739–742.

van der Valk, A., Warner, B., 2009. The development of patterned mosaic landscapes: an overview. Plant Ecol. 200, 1–7.

Vance, R.R., 1984. Interference competition and the coexistence of two competitors on a single limiting resource. Ecology 65, 1349–1357.

von Hardenberg, J., Kletter, A.Y., Yizhaq, H., Nathan, J., Meron, E., 2010. Periodic versus scale-free patterns in dryland vegetation. Proc. Roy. Soc. B 277, 1771–1776.